Seismic performance evaluation of steel moment resisting frames with mid-span rigid rocking cores

Ali Akbari
Department of Civil Engineering, Faculty of Engineering, Kharazmi University, Tehran, Iran
https://orcid.org/0000-0003-4334-579X
Ali Massumi (massumi@khu.ac.ir)
Department of Civil Engineering, Faculty of Engineering, Kharazmi University, Tehran, Iran
Mark Grigorian
MGA Structural Engineering Consultants Inc., Glendale, California, USA

Research Article

Keywords: Rocking core, Self-centering, Seismic performance, Incremental dynamic analysis

Posted Date: November 7th, 2022

DOI: https://doi.org/10.21203/rs.3.rs-2231508/v1

Seismic performance evaluation of steel moment resisting frames with mid-span rigid rocking cores

Ali Akbari[a], Ali Massumi[a,*] Mark Grigorian[b]

[a] Department of Civil Engineering, Faculty of Engineering, Kharazmi University, Tehran, Iran
[b] MGA Structural Engineering Consultants Inc., Glendale, California, USA

Abstract

The combination of replaceable and repairable properties in structures has introduced new approach called "Low Damage Design Structures". These structural systems are designed in such a way that through self-centering, primary members and specific connections neither suffer damage nor experience permanent deformations after being exposed to severe earthquakes. The purpose of this study is the seismic assessment of steel moment resisting frames with the aid of rigid rocking cores. To this end, three steel moment resisting frames of 4-, 8-, and 12-story buildings with and without rocking cores were developed. The nonlinear static analysis and incremental dynamic analysis were performed by considering the effects of the vertical and horizontal components of 16 strong ground motions, including far-fault and near-fault arrays. The results reveal that rocking systems benefit from better seismic performance and energy dissipation compared to moment resisting frames and thus structures experience a lower level of damage under higher intensity measures. The analyses show that the interstory drift in structures equipped with stiff rocking cores is more uniform in static and dynamic analyses. A uniform interstory drift distribution leads to a uniform distribution of the bending moment and a reduction in the structure's total weight and future maintenance costs.

Keywords: Rocking core, Self-centering, Seismic performance, Incremental dynamic analysis

1. Introduction

Civil engineering infrastructures may experience severe damage during earthquakes. However, based on seismic codes, their overall stability must be maintained without causing any significant casualties [1]. Accordingly, after a severe ground motion, the structure will be seriously damaged; it experiences a considerable reduction in its performance level as well as its ideal operational usage and serviceability. Reconstructing damaged structures usually demands enormous costs. This creates critical dilemmas in populated cities; because an enormous group of people may lose their jobs and residences for an extended period [2]. Since repairing the damage is not cost-effective, demolishing damaged structures and constructing new buildings is inevitable. However, this makes it challenging to accommodate earthquake victims and it also requires spending large amount of money on temporary accommodations and reconstruction of new structures. To reuse structures in the future, it is essential to conduct rehabilitation and maintenance actions but these measures may not be financially viable in some cases [3,4].

---

* Corresponding author: Ali Massumi, Professor of Structural Engineering, Kharazmi University

E-mail address: massumi@khu.ac.ir

Tel.: +98 88830891, Fax: +98 86072732

ORCID iD: 0000-0003-4636-6553

Over the course of decades, earthquakes caused unforgettable disasters along with huge detriments captured in history. For instance, the 2008 Wenchuan earthquake killed more than 86000 people and caused about \$138.33 billion financial losses. The Great Kobe earthquake killed 6434 people and caused economic damage of about \$170 billion [2]. Hence, engineers pondered about state-of-the-art systems so as to reduce the effects of earthquakes.

In a broad sense, seismic design codes aim to dissipate lateral forces' energy by using plastic deformation characteristics of members. Although plastic joints are considered as the essence of irreparable damage, structures designed with this property suffer a great deal of damage while they are subjected to a severe seismic excitation [5]. In these situations, structures experience residual drifts, thereby the predefined performance level would not be reached and in some cases, considerable reconstruction costs would be required. The input energy in conventional structures induced by an earthquake is absorbed by primary elements, including beams and columns or lateral load-bearing systems such as braces and shear walls. Consequently, researchers have always pursued new approaches to address this need for repairable structures [6]. To address the aforementioned problems, researchers have always been looking for new ways to limit the applied ground energy to the structure during an earthquake or dissipate this energy in non-structural components. In recent years, with the development of science and technology, new methods for seismic design of structures based on damage-based design concepts have been developed. These methods have improved the life safety and collapse prevention performance levels in the construction process.

One of the modern perspectives for enhancing the seismic performance of structures is using the low-damage design approach [7] which reduces the interstory drift ratio and conducts damage to certain predetermined members. In these structures, it is possible to easily replace the damaged components and enhance the system's serviceability after a significant seismic event [3]. Amongst the low-damage structural systems, structures with rocking cores that include relatively rigid cores, link beams, post-tension cables, and fuse elements are noted. In addition to high functionality, energy dissipation, and reduction of probable damage, these systems cause less residual displacements in structures. They are designed in such a way that through self-centering, primary members and specific connections neither suffer damage nor experience permanent deformations after being exposed to severe earthquakes. In this case, buildings can readily operate by affordable and replaceable damaged fuses. In these systems, the main structure behaves completely elastic, and energy absorption and inelastic performance only occur in predetermined elements [8,9].

For the first time, Housner [10] concluded that rocking motion was the critical factor preventing high-rise buildings from failures. Hucklebridge and Clough [11] carried out an experimental investigation on a 3-story steel frame. They noted that the uplifting in the columns diminished the lateral displacement and seismic forces compared to similar structures with restrained supports. In 2001, the precast post-tensioned structural shear wall systems were examined by Rasterpo et al. [12]. It was observed that by applying a large lateral force, an empty space was created at the foot of the wall, which consequently imposed a large compressive strain at the corner of it. In 2017, Lou et al. [13] introduced a new form of prestressed shear walls with horizontal bottom slits that were placed symmetrically at the wall-foundation interface. The concrete in the middle of the wall width remained connected with the foundation. Additionally, unbonded prestressed tendons were adopted to provide self-centering ability. Mohammadi et al. [14] assessed the seismic performance of reinforced concrete structures with fixed and hinged base connections. The test results denoted that hinged support frames with base-level beams had a better seismic behavior compared to fixed support frames. Moreover, the base-level beams could be considered as replaceable components which provide the repairability of structures. Gregorian et al. [15] proposed a new system consisting of moment frames connected to concrete rocking walls through story-level rigid links. The results showed the new system tended to bend similar to a straight simply supported beam with minimal drift and prevented soft story formation within the moment frame. It could also prevent severe damage to its columns and footings and recentered itself afterward. In 2018, Massumi et al. [16] examined the effects of opening geometry and its location on the seismic performance of steel shear walls. Several shear walls with various types of openings area were modeled. The analyses results showed that both the shape and the location of the openings significantly affected the seismic behavior of the prototypes; as the opening getting closer to the columns, the stiffness and strength of the system increased. Blebo and Roke [17] developed a pin-supported self-centering rocking core system with buckling-restrained columns at the first story external column positions. The seismic performance of the system was assessed by using several earthquake records. The analysis results showed high ductility and effectiveness of this seismic-resistant system. Hu et al. [18] examined the effect of various factors such as changing the initial force or the elastic stiffness of post-tensioned tendon on the dynamic response of self-centering walls. In 2019, Lin et al. [19] introduced the curved-base rocking walls and explored the advantages of this geometric modification on the behavior of timber buildings. In another study, Wu et al. [20] investigated the effect of three dimensionless parameters on the dynamic behavior of a full-size structural system. It was concluded that the modal damping ratios were significantly affected by these three parameters. Blomgren et al. [21] investigated the seismic performance of a cross-laminated timber rocking shear wall system. The prototype wall system was subjected to several ground motion records. It was designed to remain undamaged during frequent service level earthquakes and repairable after more significant events. The test results demonstrated that the proposed system was able to attain the expected seismic performance. In 2020, Xie et al. [22] evaluated the hysteretic performance of self-centering buckling-restrained braces with friction fuses. The prototypes were analyzed through a quasi-static test. The results indicated that activation of the friction fuse could efficiently increase the deformation capacity of the brace. Li et al. [23] proposed a practical seismic design approach consisting of self-centering panels and steel strip braces. The nonlinear time history analyses were performed. It was found that the considered system designed using the proposed approach could meet the requirements specified for the selected performance objectives. Li et al. [24] have recently developed a self-centering steel-timber hybrid shear wall composed of a post-tensioned steel frame and an infill light-frame wood shear wall. Experimental results revealed a peculiar flag-shaped hysteretic behavior in the proposed system. The energy dissipation behavior of the system was transferred from the plasticity in primary structural members to the frictional dissipation in the dampers, and the residual deformation of the system was controlled effectively. Hu et al. [25] focused on developing a performance-based design procedure for self-centering energy-absorbing dual rocking core systems. According to the results, it was observed that the systems designed through the proposed displacement-based design method could successfully obtain the desired performance target. Elettore et al. [26] investigated a type of self-centering damage-less steel column base connection used within steel moment resisting frames. The proposed connection consisted of a rocking column equipped with a combination of friction devices and post-tensioned bars with disk springs. The results showed the proposed system was effective in reducing the residual story drifts and protecting the first-story columns from damage.

In self-alignment and repairable systems, the system's ability to realign itself after a major seismic event is as essential as its capacity to resist the same event without any collapse. The scope of the current paper is limited to the seismic performance assessment of the steel moment resisting frame with and without a rigid rocking core in order to collapse prevention. So, in this study, the interstory drift ratio is considered as the main damage index. But the effect of recentering on enhancing the structural performance is neglected.

This paper aims to assess the seismic performance of steel moment resisting frames equipped with rigid rocking cores installed on the mid-span of the frames. It also evaluates the effects of height change on the seismic performance of structures. To this end, some steel frames were initially designed and modeled according to the current regulations. Then the rocking core system was added to the mid-span of the designed frames. Next, the frames were analysed using nonlinear static and dynamic analyses. The seismic responses of the rocking systems and ordinary frames were then determined, and eventually, the obtained results were discussed.

This paper is organized as follows: section 2 introduces the models used in the research; the details of modeling, and the assumptions governing them. Furthermore, the verification of numerical models in OpenSees [27] is presented in this section too. In section 3, the ground motions used in the nonlinear time history analysis are presented. The last section, section 4, is devoted to nonlinear static and dynamic analyses and the results are discussed.

2. Methodology

2.1. Verification of numerical models

Concerning the verification of the numerical models and analysis results, the research model investigated by Qu et al. [28] was used in this study. This model is a 3-story and 4-span steel frame with the properties summarized in Table 1. The steel grades of beams and columns are A36 and A572Gr50, with the yielding stress of 248 MPa and 345 MPa, respectively. All sections are made of fiber; a force-based element is practiced so as to model beams and columns. A rigid truss element is used to model the links connecting the moment frame to the stiff rocking core and an elastic beam element is assigned to model the rocking core. The applied loads are consistent with Gupta and Krawinkler's paper [29]. Figure 1 illustrates the frame configuration.

Table 1. Design of the 3-story frame [28]

Story	Column		Beam
	External	Internal	
1	W14×257	W14×311	W33×118
2	W14×257	W14×311	W30×116
3	W14×257	W14×311	W24×68

Modal analysis was done at first to verify the modal properties of frames in the linear state. The result shows a slight difference between the fundamental period of Qu et al. and this study model (about 2% error), indicating the adequacy of this model. Then, the nonlinear behavior was examined with the aid of nonlinear static analysis. It was proven that modeling was benefited from acceptable accuracy, as exhibited in Figure 2.

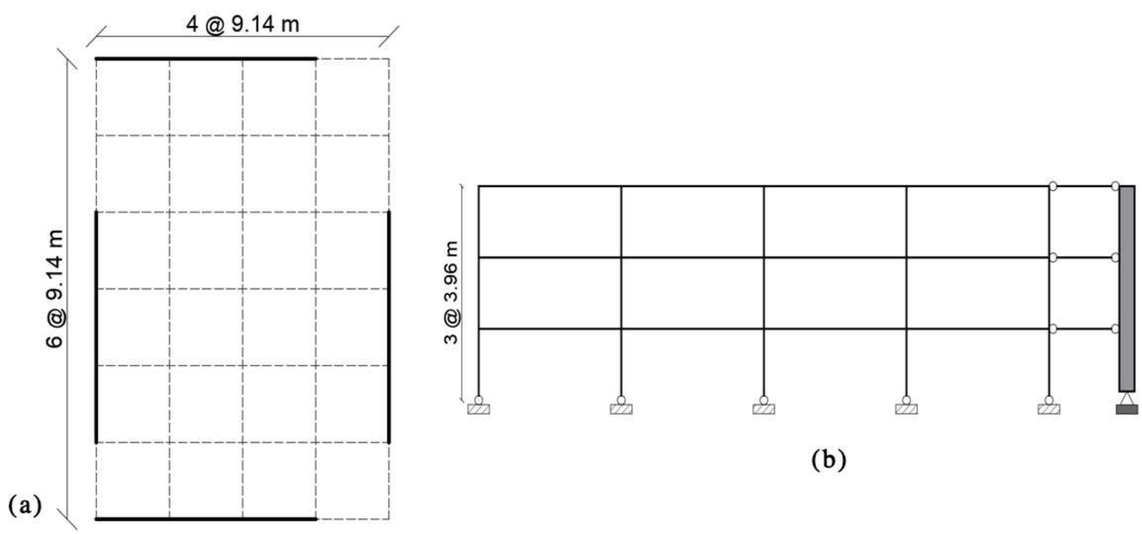

Figure 1. (a) Plan view and (b) elevation view of the 3-story structure [28]

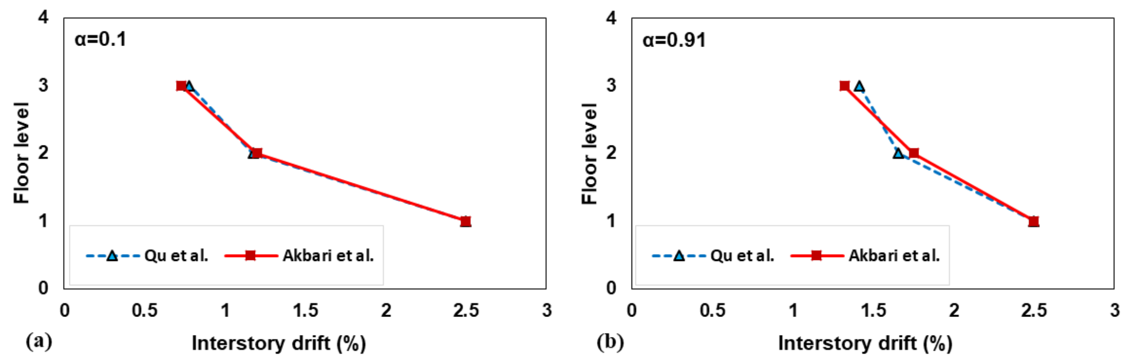

Figure 2. Interstory drift of the 3-story frame at (a) stiffness ratio=0.1, and (b) stiffness ratio=0.91

Figure 2 shows the performance of the rehabilitated system based on relative stiffness of rocking core, α, given by Eq. (1):

$$\alpha = \frac{EI_{RC}}{k_1 h_{s1}^3} \qquad (1)$$

where E denotes elasticity modulus of the rocking core material, I_{RC} is the moment of inertia of the rocking core, k_1 and h_{s1} are the elastic stiffness and the height of the considered structure's first story, respectively. The new suggested walls were added to the verified models after ensuring the structures exhibit roughly the same nonlinear behavior.

2.2. Numerical modeling of rocking systems

OpenSees software was used for numerical modeling and analysis involved in the current study.The Giuffre-Menegotto-Pinto steel model with isotropic strain hardening (Steel02) and linear tension softening concrete model (Concrete02) was assigned to the steel frame members and pinned support concrete shear wall. It is assumed that the steel material had a mean yield strength of 240 MPa, and a strain hardening ratio of 1%. The compressive strength of concrete used to represent the behavior of concrete shear wall was 27.6 MPa. Moreover, A416Gr270 was used to design the post-tensioned cables with a mean yield strength of 1690 MPa and Young's modulus of 196500 MPa.

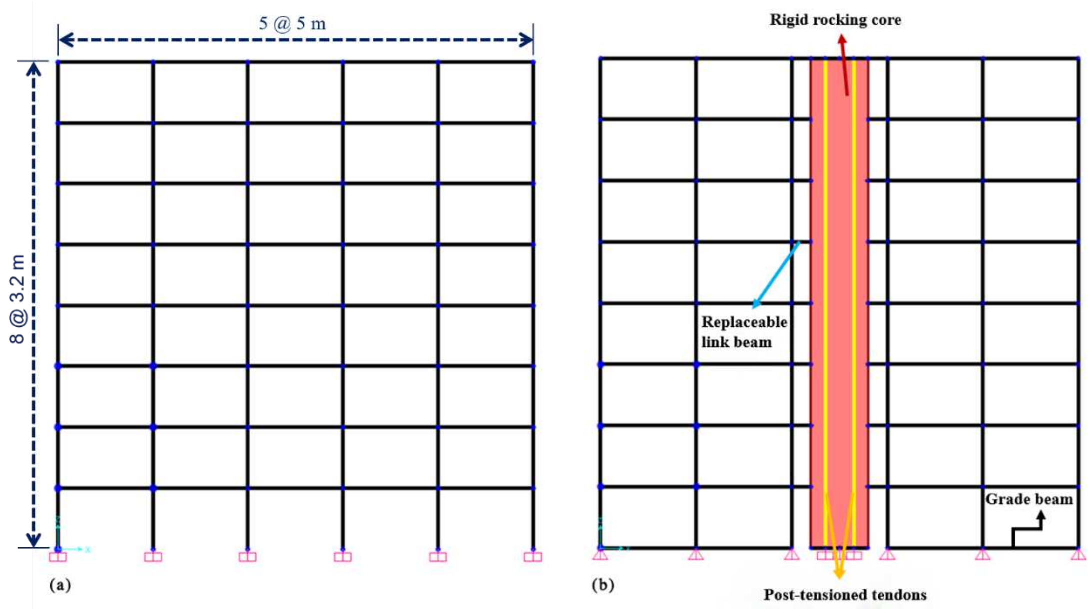

Figure 3. Prototypes configuration of (a) conventional steel moment frame, and (b) frame with the mid-span rigid rocking core

A nonlinear beam column element with ten integration points along its longitudinal direction is assigned to beam and column elements. A truss element is practiced to model pin-ended link beams connect the steel moment frame to the stiff rocking core, and post-tensioned cables. A displacement-based beam-column element is used to model the stiff concrete rocking wall with wide column method. The schematic configuration of models is depicted in Figure 3.

2.3. Design

In the present study, three different steel frames of 4, 8, and 12 stories were designed based on AISC 360-10 [30] and the Iranian seismic code [31]. It is assumed that all the structures are located in a region of high seismicity and lying on soil type II, corresponding to very dense soil or soft rock. Noteworthy, the specifications of the structures have been selected so that they are comparable with the conventional building frames. All frames are two-dimensional and have five bays of 5 m width. The height of each story is 3.2 m; since the stiff rocking core is installed on a side of the frame, it has a loading width of 2.5 m. The elevation view and plan view of 4-, 8- and 12-story buildings are illustrated in Figure 4.

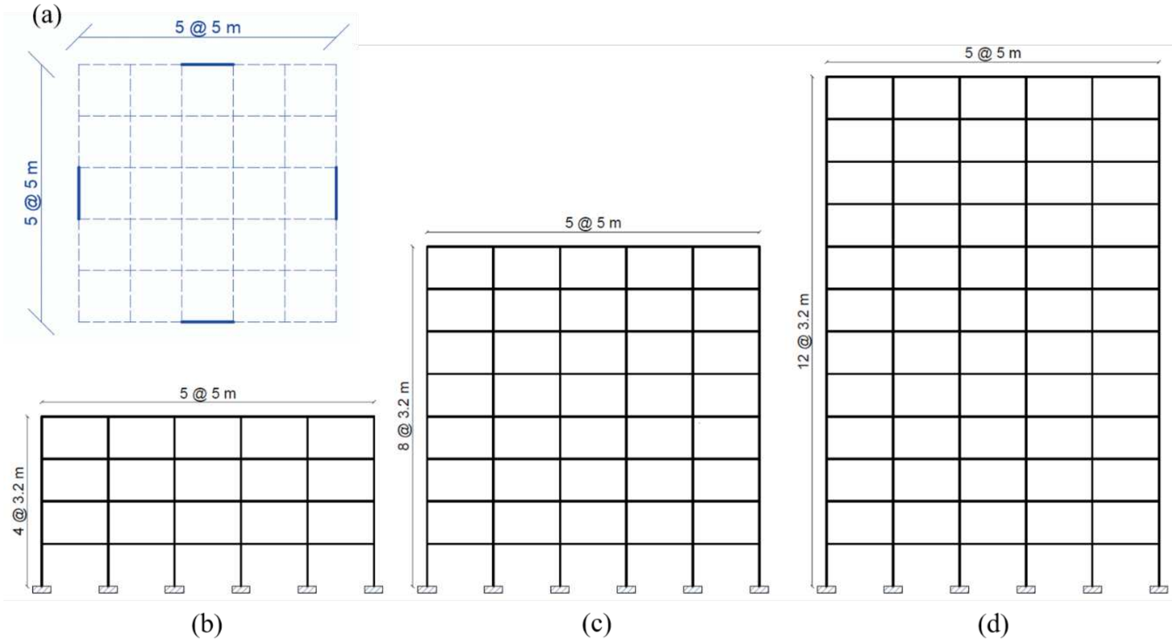

Figure 4. (a) Schematic plan view of models, and elevation view of (b) 4-story building, (c) 8-story building, and (d) 12-story building

The gravity loads for all structures are constant. The story dead and live loads are assumed to be 5.1 kN/m2 and 1.96 kN/m2, respectively; the roof live load is also 1.47 kN/m2 [32]. Traditional steel moment resisting frames and frames with the rocking system are hereafter denoted X-st and X-st-R, respectively. Figure 5 shows the detailed configuration of the rocking cores, and the frame sections details are depicted in Table 2.

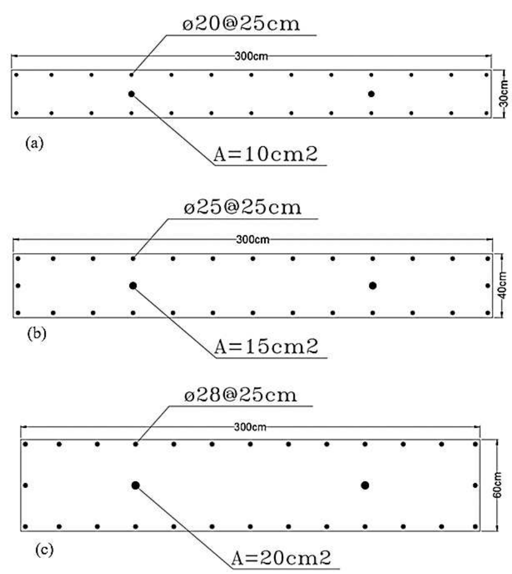

Figure 5. Rocking core configuration of (a) 4-story frame, (b) 8-story frame, and (c) 12-story frame

Table 2. Designed element sections of the considered models

Model	Story number	Beam	Column	Rocking wall (m × m)	Wall reinforcement
4st	1-2 3-4	W14×68 W14×53	W14×99 W14×90	-	-
4st-R	1-2 3-4	W14×68 W14×53	W14×99 W14×90	3 × 0.3	26 Ø20
8st	1 2 3 4 5-7 8	W14×82 W14×99 W14×90 W14×82 W14×68 W14×38	W14×132 W14×133 W14×99 W14×99 W14×90 W14×90	-	-
8st-R	1 2 3 4 5-7 8	W14×82 W14×99 W14×90 W14×82 W14×68 W14×38	W14×132 W14×133 W14×99 W14×99 W14×90 W14×90	3 × 0.4	28 Ø25
12st	1 2-3 4 5-6 7-8 9-10 11-12	W14×90 W14×109 W14×109 W14×90 W14×82 W14×68 W14×38	W14×193 W14×193 W14×132 W14×132 W14×90 W14×90 W14×90	-	-
12st-R	1 2-3 4 5-6 7-8 9-10 11-12	W14×90 W14×109 W14×109 W14×90 W14×82 W14×68 W14×38	W14×193 W14×193 W14×132 W14×132 W14×90 W14×90 W14×90	3 × 0.6	28 Ø28

3. Ground motions selection

Since structures exhibits various behaviors under different earthquake excitation, selecting proper ground motions becomes highly significant with regards to the nonlinear time history analysis. Hence, by choosing a wide range of ground motions, a comprehensive evaluation of the structure's behavior is made. To this end, a set of 16 ground motion pairs from the online ground motion database of the Pacific Earthquake Engineering Research Center [33] was selected. It consists of eight far-fault and eight near-fault records chosen in accordance with the aforementioned site conditions of the study cases. The basic specifications of each ground motion are summarized in Table 3 and Table 4.

Table 3. Basic characteristics of near-fault earthquake records

RSN	Event	Station Name	Magnitude	R_{rup} (km)	PGA_X (g)	PGA_Z (g)	PGVx (cm/s)
139	Tabas_ Iran	Dayhook	7.35	13.94	0.32	0.19	22.30
292	Irpinia, Italy-01	Sturno (STN)	6.90	10.84	0.23	0.23	36.98
779	Loma Prieta	LGPC	6.93	3.88	0.57	0.90	96.10
828	Cape Mendocino	Petrolia	7.01	8.18	0.59	0.17	49.33
864	Landers	Joshua Tree	7.28	11.03	0.27	0.18	27.02
1507	Chi-Chi, Taiwan	TCU071	7.62	5.80	0.53	0.42	52.30
1633	Manjil_ Iran	Abbar	7.37	12.55	0.51	0.54	42.46
1787	Hector Mine	Hector	7.13	11.66	0.27	0.15	26.01

Table 4. Basic characteristics of far-fault earthquake records

RSN	Event	Station Name	Magnitude	R_{rup} (km)	PGA_X (g)	PGA_Z (g)	PGVx (cm/s)
15	Kern County	Taft Lincoln School	7.36	38.89	0.16	0.11	15.23
70	San Fernando	Lake Hughes #1	6.61	27.40	0.15	0.11	18.16
212	Livermore-01	Del Valle Dam (Toe)	5.80	24.95	0.13	0.07	11.65
288	Irpinia, Italy-01	Brienza	6.90	22.56	0.22	0.20	13.10
359	Coalinga-01	Parkfield - Vineyard Cany 1E	6.36	26.38	0.18	0.08	17.95
472	Morgan Hill	San Justo Dam (R Abut)	6.19	31.88	0.08	0.04	7.64
572	Taiwan SMART1(45)	SMART1 E02	7.30	51.35	0.14	0.05	14.43
897	Landers	Twentynine Palms	7.28	41.43	0.08	0.04	3.62

The selected ground motions cover a magnitude range from 5.5 to 7.5 and a rupture distance range from 0 to 15 km for near-fault and 20 to 55 km for far-fault earthquakes [34]. Figure 6 shows the horizontal and vertical components of earthquake accelerograms with a magnitude more than 7.30 used in this study.

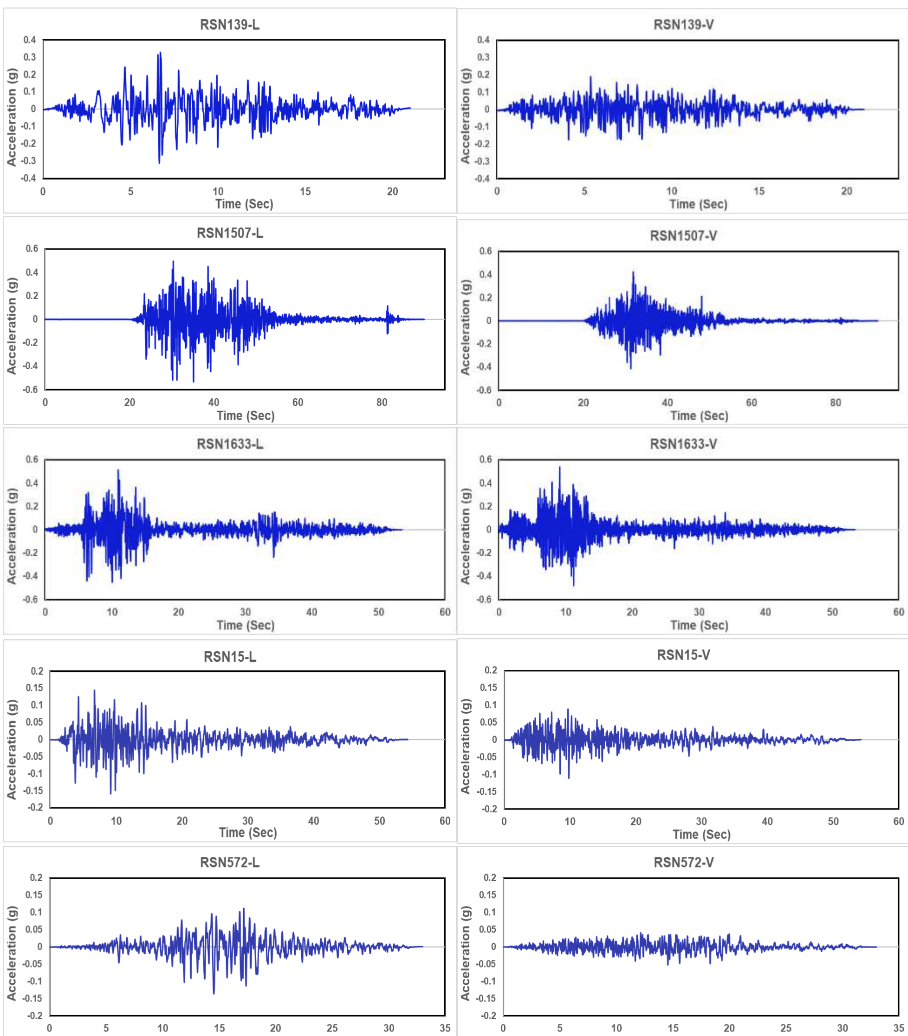

Figure 6. Longitudinal and vertical components of earthquake records with a magnitude more than 7.30

4. Results and discussions

To investigate the performance of the rigid rocking core, nonlinear static and dynamic analyses are conducted separately. The results are subsequently discussed in terms of interstory drift ratios, structural periods, base shears at the collapse prevention performance level, energy dissipation, and interstory drifts. In the following, static and dynamic analyses are illustrated in separated sections.

4.1. Nonlinear static analysis

In the first step, the structures were analyzed through nonlinear static analysis under constant gravity load coupled with inverted triangle lateral load distribution. Relying on ASCE 41-13 [35], the interstory drift limits of moment frames associated with Immediate Occupancy (IO), Life Safety (LS), and Collapse Prevention (CP) performance levels are calculated by about 0.7%, 2.5%, and 5%, respectively. The application of lateral loads is limited to a relative displacement of 5% of the structure height according to the collapse prevention level.

Concerning the pushover analysis results shown in Figure 7, it can be seen that the frames with rocking system show more strength and capacity than conventional frames. Additionally, the stiffness of rocking systems reduced by 20%, 16%, and 13% compared to the conventional 4-, 8-, and 12-story moment resisting frames, respectively. The reduced stiffness of the frames instrumented with rocking cores compared to conventional structures explains the increase in the vibration period of the first mode (Table 5). This increase is relatively the largest for the 12-story frame in comparison with the other models.

Table 5. The modal properties of frames for the first three modes

Modes	Vibration period (s)	Modal mass (%)	Vibration period (s)	Modal mass (%)	Vibration period (s)	Modal mass (%)
	4St		**8St**		**12St**	
Mode 1	0.53	83	0.94	79	1.29	76
Mode 2	0.17	12	0.32	12	0.46	12
Mode 3	0.09	4	0.18	4	0.27	4
	4St-R		**8St-R**		**12St-R**	
Mode 1	0.56	82	0.98	78	1.33	77
Mode 2	0.04	7	0.04	6	0.05	2
Mode 3	0.04	4	0.04	4	0.11	1

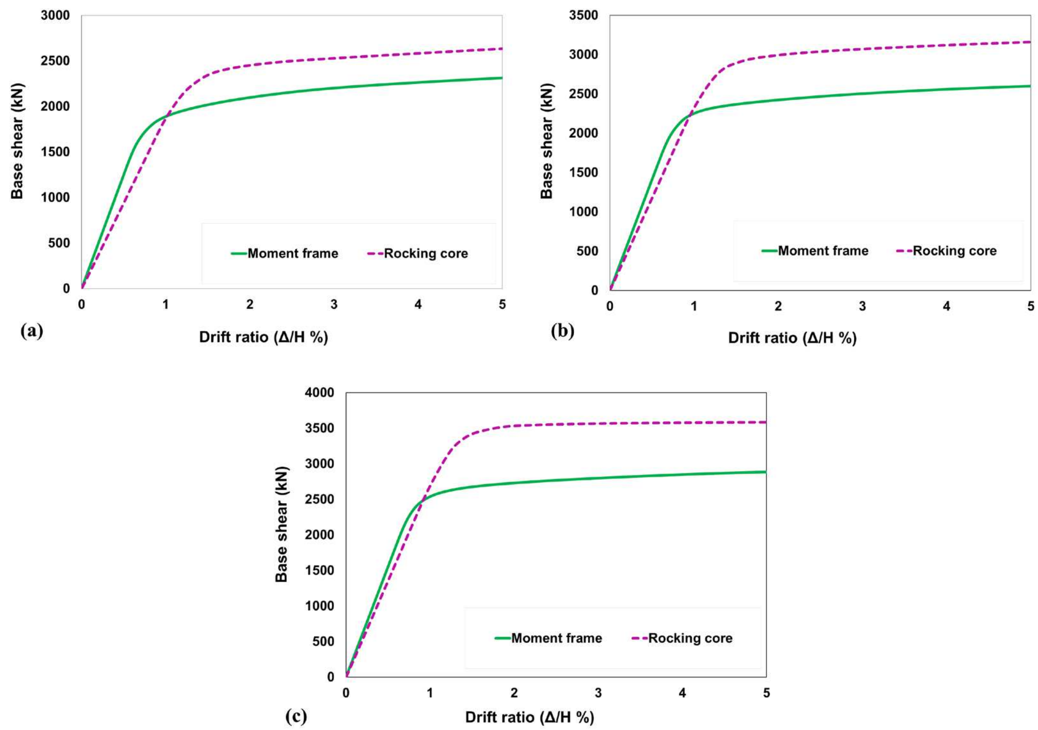

Figure 7. Pushover curves for (a) 4-story, (b) 8-story, and (c) 12-story frames with and without rocking core

According to Figure 7, the base shear of 4-, 8-, and 12-story frames instrumented with rocking cores is roughly 1.15, 1.20, and 1.25 times more than the corresponding values of the conventional structures. To evaluate the energy dissipation potential of the systems, the pushover bi-linear diagrams are extracted using Paulay and Priestley method [36], as depicted in Figure 8. The area under the curves indicates that the energy absorbed in the 4-, 8-, and 12-story frames with stiff rocking cores rises by 11%, 18%, and 23%, respectively. Ductility and overstrength factor are among the most critical parameters calculated from bi-linear diagrams. Ductility (μ) is the ratio of failure displacement (Δ_{max}) to yield displacement (Δ_y) and overstrength factor (R_s) is the ratio of maximum base shear (V_0) in actual behavior to first significant yield strength (V_s) in structure. Values for these two parameters are listed in Table 6. The reduction in ductility and overstrength factor in rocking structures compared to steel moment resisting frames can be explained by the fact that in structures equipped with rigid rocking cores, fixed supports are replaced by pinned supports and lateral load bearing is mainly done by the rocking core. Besides, it is assumed that structures collapse at 5% drift in pushover analysis.

Table 6. Data of ductility and overstrength factor

Model	Δ_y (m)	Δ_{max} (m)	V_s (kN)	V_0 (kN)	R_s	μ
4st	0.13	0.64	1475.8	2314.4	1.57	4.94
4st-R	0.18	0.64	1736.7	2635.4	1.52	3.50
8st	0.24	1.28	1500.2	2599.9	1.73	5.32
8st-R	0.35	1.28	2163.5	3161.6	1.46	3.65
12st	0.36	1.92	2114.2	2886.2	1.36	5.33
12st-R	0.51	1.92	2551.3	3588.2	1.41	3.76

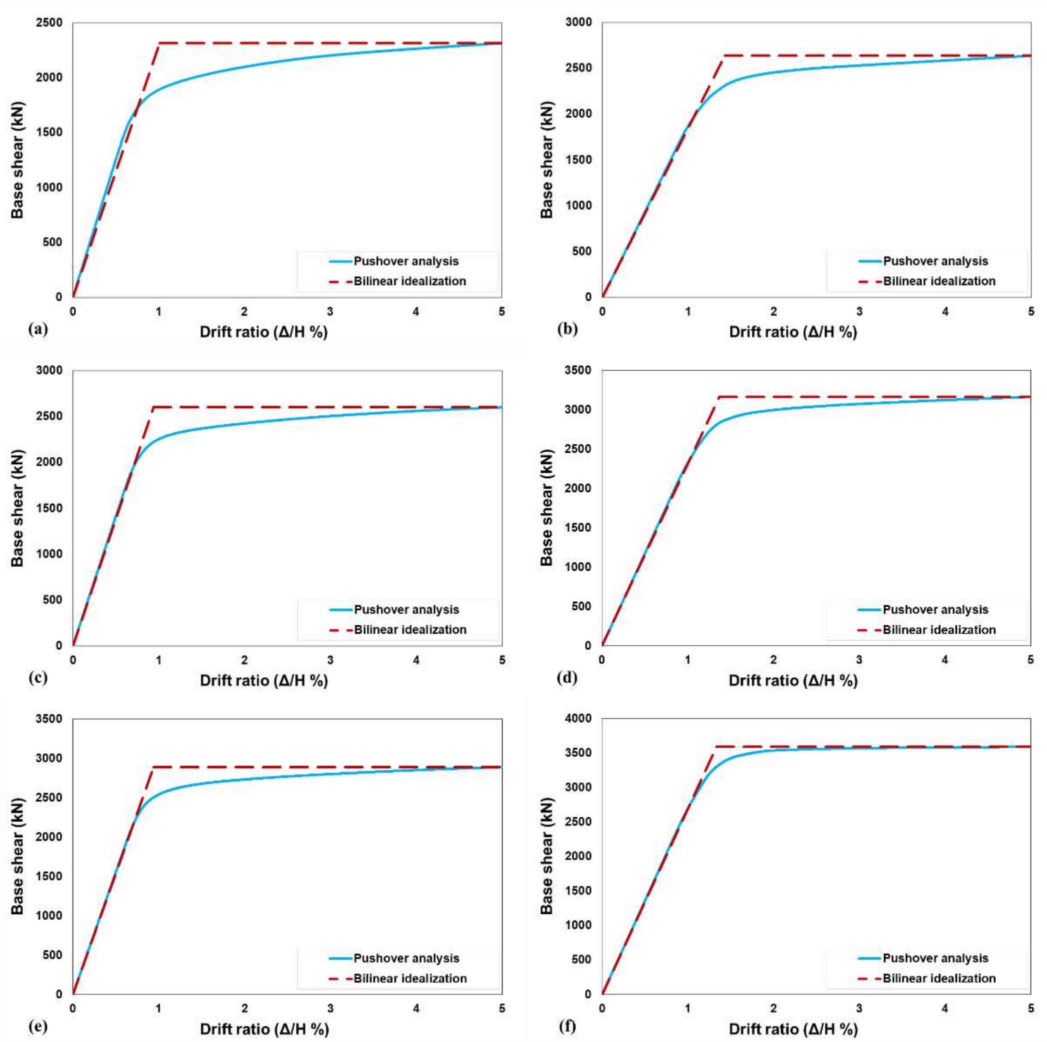

Figure 8. Pushover and bi-linear curves of (a) 4st, (b) 4st-R, (c) 8st, (d) 8st-R, (e) 12st, and (f) 12st-R

Another critical parameter calculated in this paper is the interstory drift. As can be seen in Figure 9, 4-, 8-, and 12-story moment resisting frames exhibit the interstory drift of 2.86% to 6.22%, 0.62% to 8%, and 0.68% to 8.2%, respectively. Interstory drift for rigid rocking core systems with 4 stories is 4.5% to 5.3%, with 8 stories is 4% to 5.6%, and with 12 stories is 3.9% to 5.68%. It is observed that the difference between the maximum and minimum drifts in 4-, 8-, 12-story moment resisting structures are 4.35, 4.76, and 4.25 times more than structures with rocking cores. The large difference between the maximum and minimum interstory drift values may cause soft-story failure. It is deducted that by installing rigid rocking cores, the interstory drifts are uniformly distributed compared to those in traditional moment frame systems. Thus, adding a stiff rocking core to the moment frame can prevent the formation of soft story because the relative displacements of each story become nearly similar.

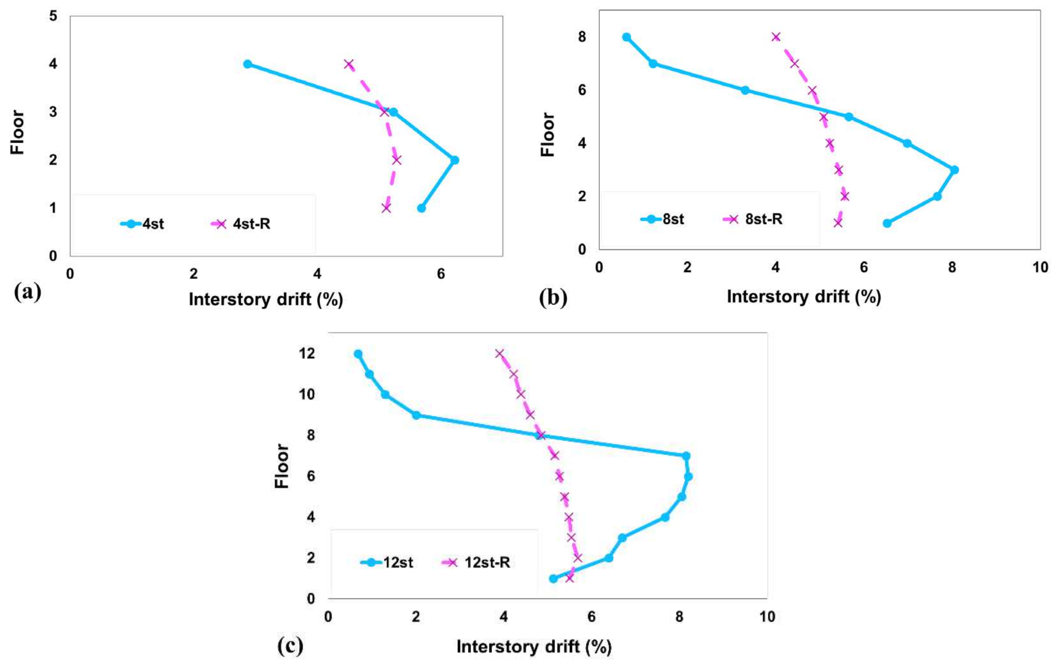

Figure 9. Interstory drifts of structures: (a) 4-story, (b) 8-story, (c) 12-story

4.2. Incremental Dynamic Analysis (IDA)

In the second step, the Incremental Dynamic Analysis (IDA) [37,38] of sixteen records, represented in section 3, is performed. An IDA curve is a plot of a Damage Measure (DM) recorded in an IDA study versus one or more intensity measures (IMs) characterizing the applied scaled accelerogram. In this study, the maximum drift ratio is supposed to be the damage measure, and the peak ground acceleration (PGA) is considered as the intensity measure. The analysis had an initial step of 0.05g with a step increment of 0.05g. As mentioned in the previous section, based on ASCE 41-13, the drift of steel moment resisting frames in IO, LS, and CP performance levels is calculated by about 0.7%, 2.5%, and 5%, respectively. So, the IDA curves are limited to a 5% drift in each structure to compare the performance of the models at the collapse point. The IDA curves of near-fault and far-fault earthquakes are shown in Figure 10 and Figure 11. Furthermore, the summarized IDA curves (16%, 50%, and 84% fractiles) are illustrated in Figure 12 and Figure 13.

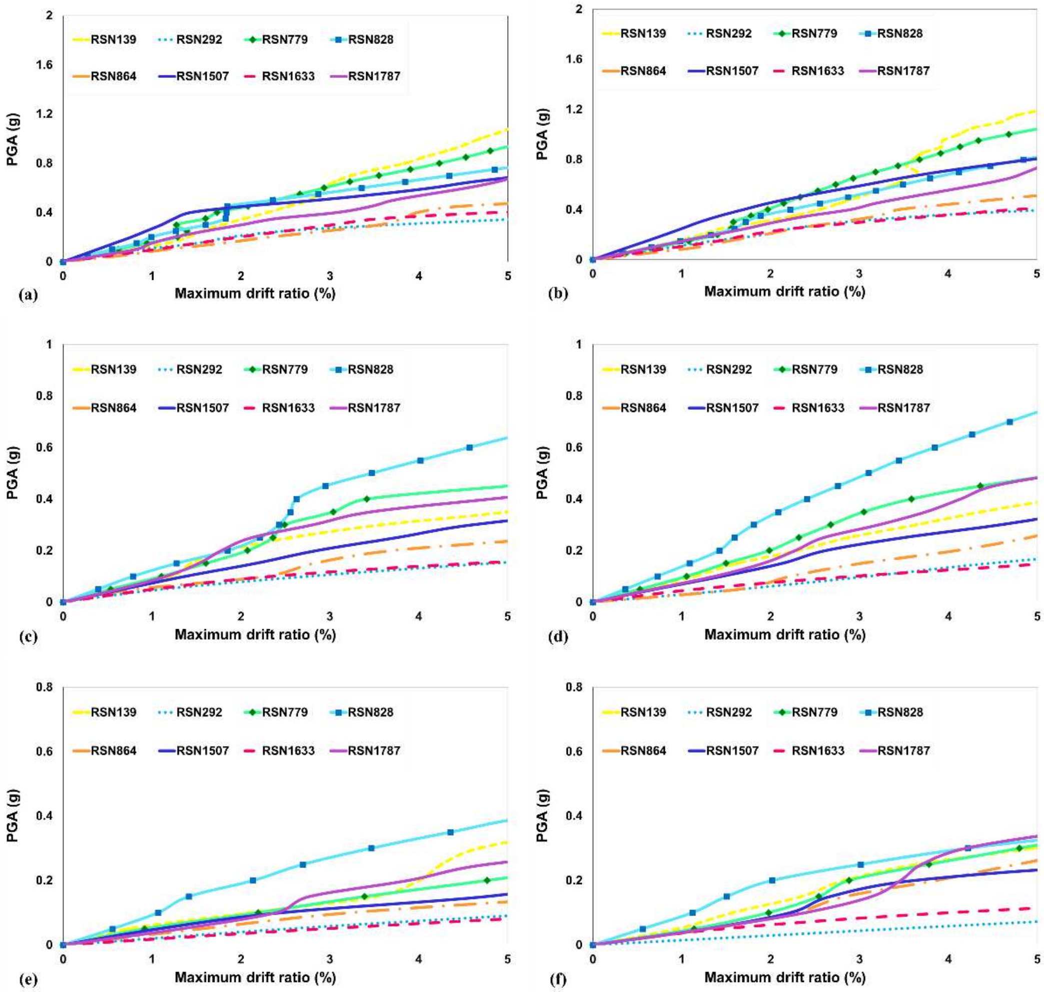

Figure 10. IDA curves for near-fault earthquakes: (a) 4st, (b) 4st-R, (c) 8st, (d) 8st-R, (e) 12st, (f) 12st-R

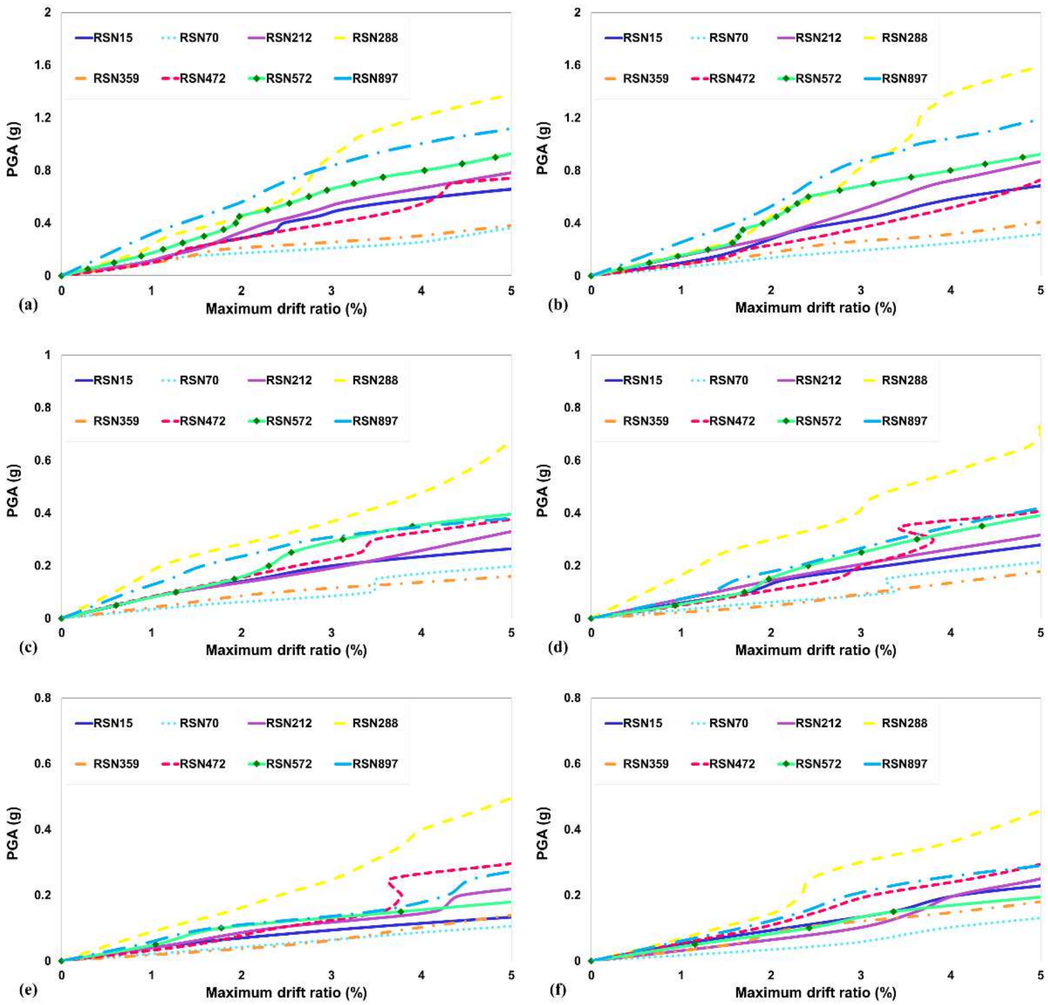

Figure 11. IDA curves for far-fault earthquakes: (a) 4st, (b) 4st-R, (c) 8st, (d) 8st-R, (e) 12st, (f) 12st-R

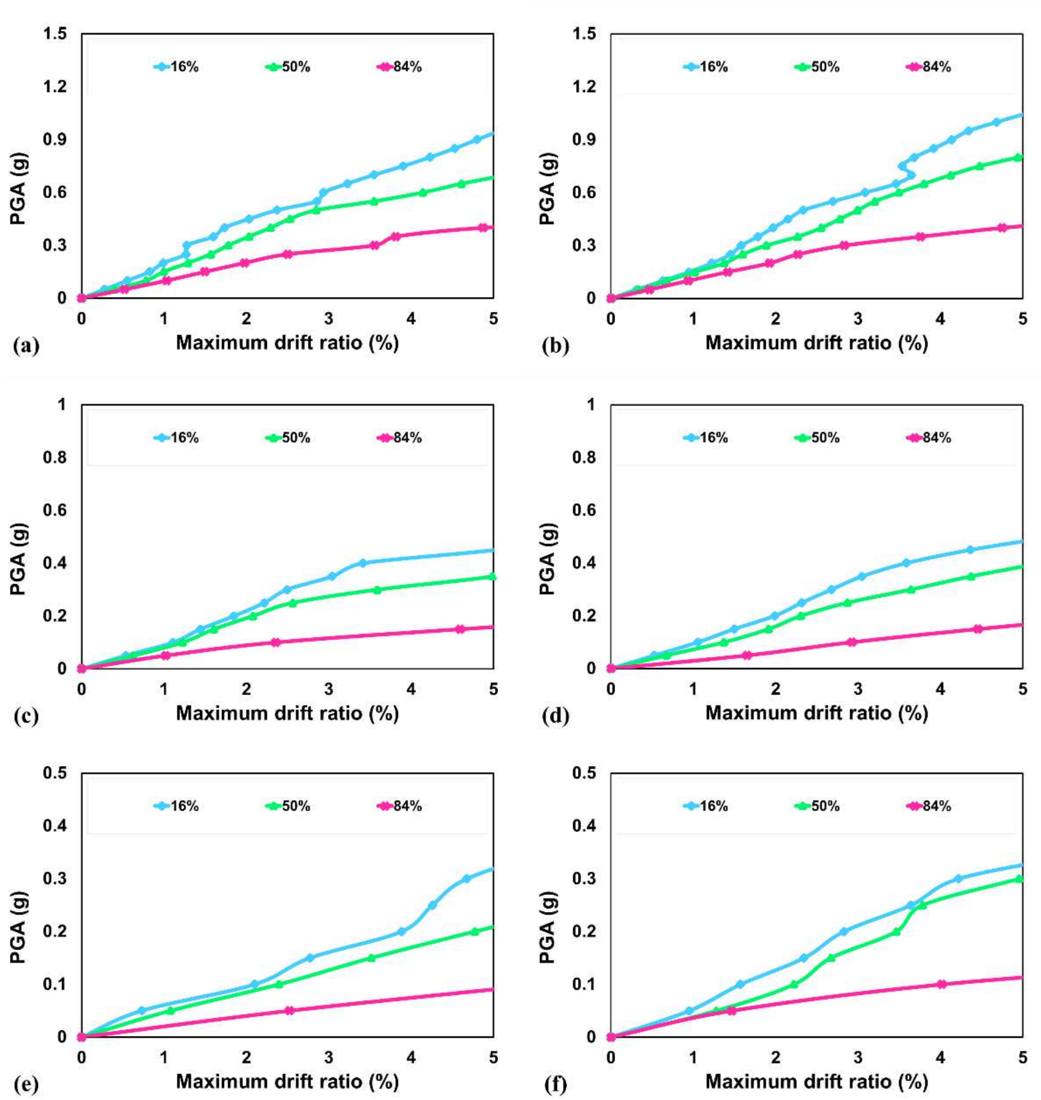

Figure 12. Summarized IDA curves for near-fault earthquakes. (a) 4st, (b) 4st-R, (c) 8st, (d) 8st-R, (e) 12st, (f) 12st-R

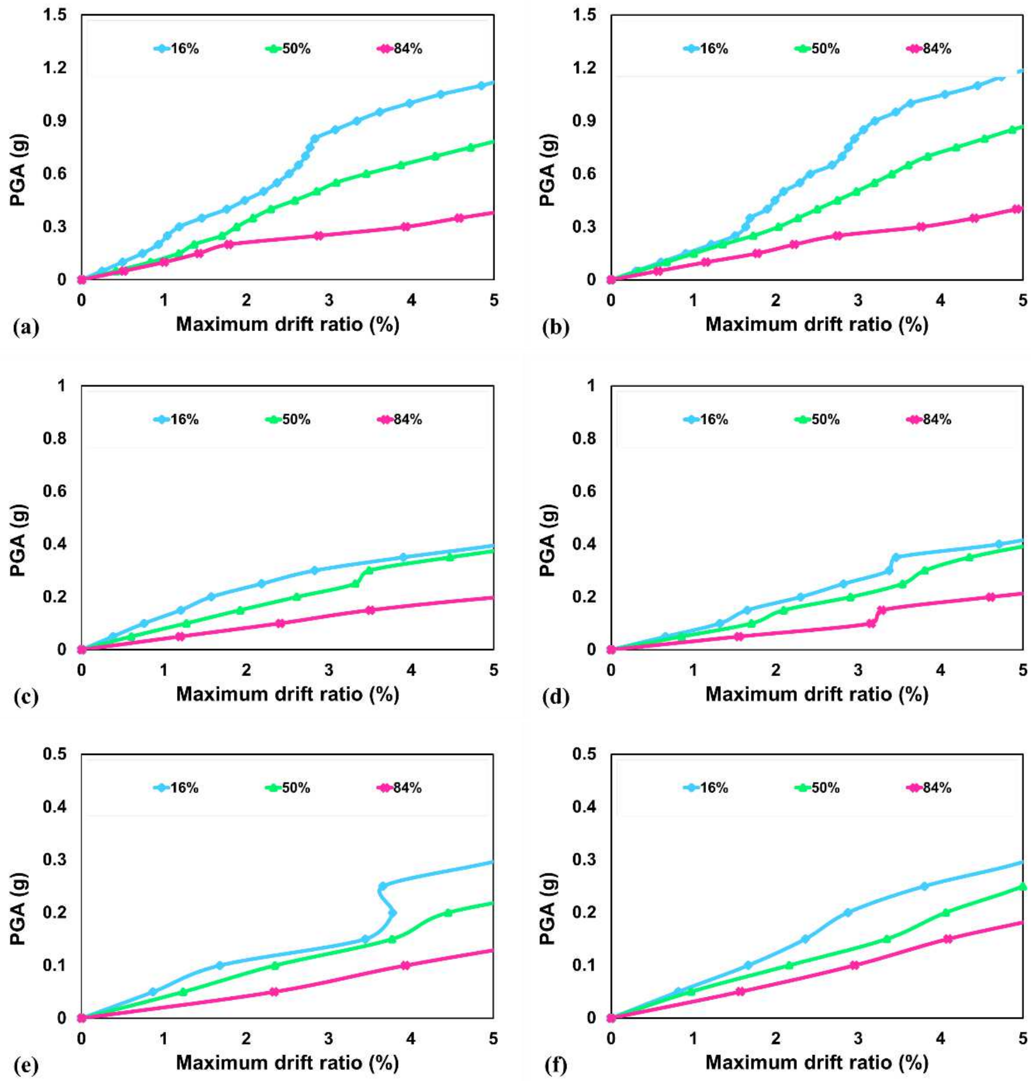

Figure 13. Summarized IDA Curves for far-fault earthquakes. (a) 4st, (b) 4st-R, (c) 8st, (d) 8st-R, (e) 12st, (f) 12st-R

A summary of peak ground acceleration at different structural performance levels for near-fault and far-fault earthquakes is presented in Table 7 and Table 8, respectively. The comparison of collapse threshold performance levels on the mean IDA curve of near-fault earthquakes indicates that the capacity has increased between 10% to 20% in all three rocking structures. Regarding far-fault earthquakes, this increase is about 15% to 20% for all systems. Besides, this increment is more significant for the 12-story frame compared to the two other structures.

Table 7. PGA corresponding to performance levels of structures for near-fault earthquake records

PGA (g)	4st			4st-R		
	16%	50%	84%	16%	50%	84%
CP=5%	0.95	0.65	0.45	1.05	0.85	0.45
LS=2.5%	0.50	0.45	0.25	0.55	0.45	0.25
IO=0.75%	0.20	0.15	0.10	0.20	0.20	0.10
PGA (g)	8st			8st-R		
	16%	50%	84%	16%	50%	84%
CP=5%	0.45	0.35	0.15	0.50	0.40	0.15
LS=2.5%	0.30	0.25	0.10	0.30	0.25	0.10
IO=0.75%	0.05	0.05	*	0.05	0.05	*
PGA (g)	12st			12st-R		
	16%	50%	84%	16%	50%	84%
CP=5%	0.35	0.20	0.10	0.35	0.30	0.10
LS=2.5%	0.15	0.10	0.05	0.20	0.15	0.05
IO=0.75%	0.05	*	*	0.05	*	*

* The PGA is less than 0.05g

Table 8. PGA corresponding to performance levels of structures for far-fault earthquake records

PGA (g)	4st			4st-R		
	16%	50%	84%	16%	50%	84%
CP=5%	1.10	0.70	0.45	1.20	0.90	0.45
LS=2.5%	0.60	0.45	0.25	0.60	0.45	0.25
IO=0.75%	0.20	0.15	0.10	0.20	0.20	0.05
PGA (g)	8st			8st-R		
	16%	50%	84%	16%	50%	84%
CP=5%	0.40	0.35	0.20	0.40	0.40	0.20
LS=2.5%	0.30	0.20	0.10	0.20	0.15	0.10
IO=0.75%	0.10	0.05	*	0.05	0.05	*
PGA (g)	12st			12st-R		
	16%	50%	84%	16%	50%	84%
CP=5%	0.30	0.25	0.15	0.30	0.25	0.15
LS=2.5%	0.15	0.10	0.05	0.15	0.10	0.05
IO=0.75%	0.05	*	*	0.05	0.05	*

* The PGA is less than 0.05g

Base shear values corresponding to various drift ratios for near-fault and far-fault earthquakes are shown in Figure 14. Considering the base shear values shown in this figure, it can be concluded that dynamic and pushover analyses follow a similar trend. Frames with rocking cores have more strength and load-bearing capacity than conventional moment frames and the stiffness of rocking structures is less than the moment frames. Besides, by comparing the areas under the curves, it is noted that the energy absorption of rocking systems has increased.

Generally, the proposed IDA curves show that structures with rigid rocking cores exhibit better seismic performance than conventional moment frames. The structures experience a specific DM at a higher IM. Moreover, the interstory drifts in rocking systems are more uniformly distributed compared with those in conventional moment frame systems.

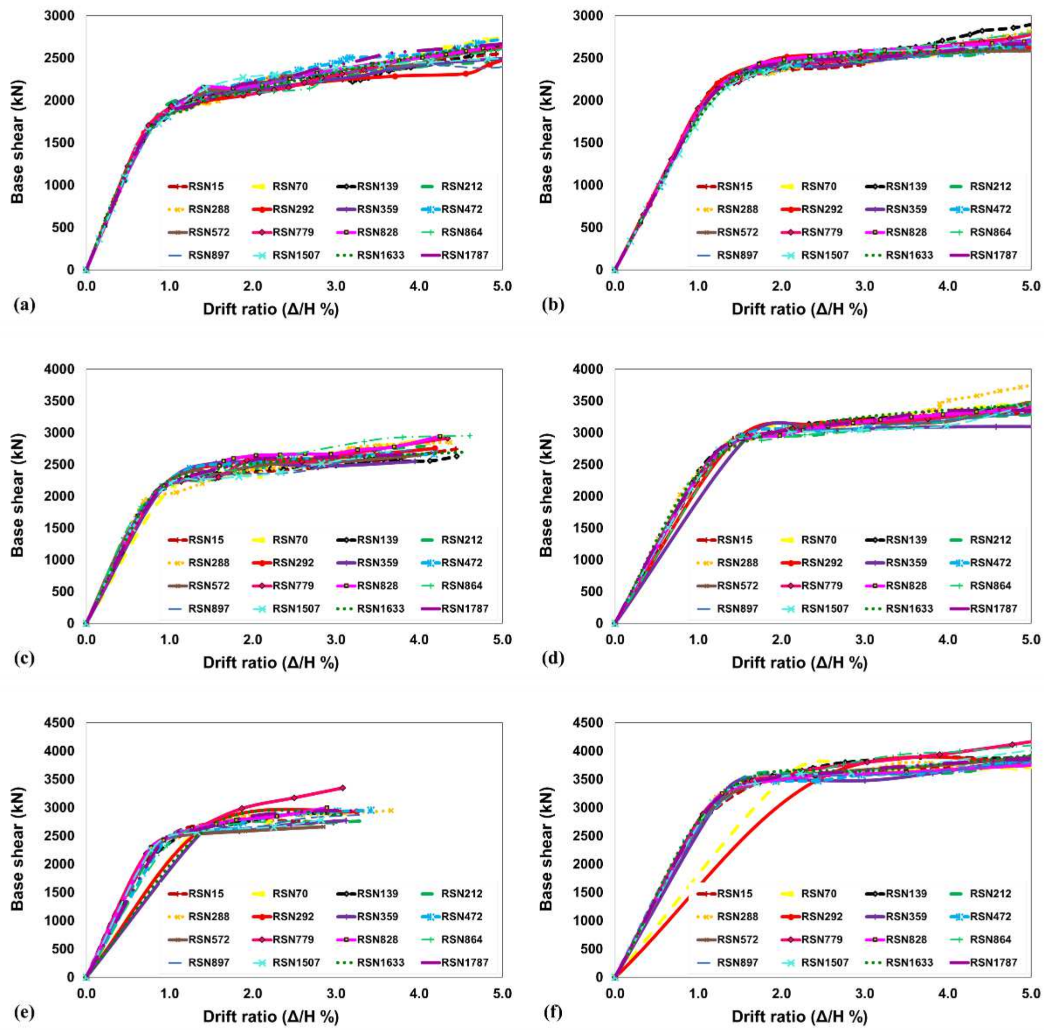

Figure 14. Comparison of base shear vs. drift ratio: (a) 4st, (b) 4st-R, (c) 8st, (d) 8st-R, (e) 12st, (f) 12st-R

Comparing the diagrams presented in Figure 12 to Figure 14 shows that near-fault earthquakes cause larger drift in the structure than far-fault earthquakes, and the structure reaches the CP level faster. Additionally, the rocking core improves the seismic performance of the structure and this improvement is more considerable in structures exposed to far-fault ground motions.

Based on the results obtained from both static and dynamic analysis, the interstory drifts are more uniformly distributed in rocking core systems than those in conventional moment frame systems. The rocking core in the mid-rise structures performs better than the low-rise structure. Besides, adding a stiff rocking core to the moment frame mitigates soft-story failure.

In comparison to fixed-base moment frame-shear walls, rocking systems can prevent the premature formation of plastic hinges at column feet and the development of failure mechanisms in structures. Therefore, there are no damaged footings or columns requiring repair; the repair work is very expensive and time-consuming. Moreover, a rocking shear wall does not suffer from footing uplift effects, toe crushing, and edge bars yielding.

On the other hand, by economically comparing rocking structures and traditional moment resisting frames, it can be seen that the use of rigid rocking cores facilitates the structural weight-reduction and confers desirable maintaining costs. Thus, this helps to save construction time and materials.

In addition, the uniform displacement distribution of the interstory drift not only results in a uniform distribution of bending moment in the members but also leads to a reduction in the total weight of the structure and, consequently, the future costs. Therefore, it allows the builders to use repetitive beams, columns, braces, and connections, enhancing structures' constructability.

It is also concluded that the sustainability of rocking structures, in which damage is conducted to limited and specific replaceable elements, helps to increase the life cycle and decrease the repairing cost of these structures after an earthquake; these factors make rocking structures more cost-effective compared to traditional structural systems.

5. Conclusions

This study aimed to compare the seismic responses of steel moment resisting frames with and without rigid rocking cores. Three different steel frames of 4, 8, and 12 stories and 5-meter spans have been designed, and the rocking cores have been added to them. The designed frames have been analyzed using nonlinear static analysis and IDA with sixteen records of far-fault and near-fault earthquakes. The following results have been obtained:

- Adding a rigid rocking core to the steel moment frame increases both the energy absorption and energy dissipation of the moment frame. It also enhances the seismic performance level of the structure. Compared to moment frames, the capacity of rocking frames in 4-, 8-, and 12-story structures increase by 11%, 18%, and 23%, respectively.
- Adding a stiff rocking core to the moment frame and changing the fixed supports to pinned supports reduce the stiffness of 4-, 8-, and 12-story structures by 25%, 20%, and 15%, respectively; this stiffness reduction causes 5% increase in the fundamental period of all three structures.
- Adding a rigid rocking core to the moment frame and changing the fixed supports to pinned supports increase the strength of the 4-, 8-, and 12-story structures by 15%, 20%, and 25 %, respectively.
- The interstory drift in structures equipped with rocking cores is uniform in both static and dynamic analysis and adding a rigid rocking core to the moment frame may prevent the formation of soft story.
- Adding a stiff rocking core to low- and mid-rise buildings where the effect of higher modes of vibrations is not considerable improves the seismic performance of structures. In the case of high-rise buildings where higher modes play a significant role in the seismic responses of structures, the use of these systems needs more investigation.

References

[1] Seismic Evaluation and Retrofit of Existing Buildings, in: Seism. Eval. Retrofit Exist. Build., American Society of Civil Engineers, 2017. https://doi.org/10.1061/9780784414859.

[2] J. Wang, H. Zhao, High Performance Damage-Resistant Seismic Resistant Structural Systems for Sustainable and Resilient City: A Review, Shock Vib. 2018 (2018). https://doi.org/10.1155/2018/8703697.

[3] M. Kafaeikivi, D.A. Roke, Q. Huang, Seismic performance assessment of self-centering dual systems with different configurations, Structures. 5 (2016) 88–100. https://doi.org/10.1016/j.istruc.2015.09.004.

[4] M. Grigorian, C. Grigorian, An introduction to the structural design of rocking wall-frames with a view to collapse prevention, self-alignment and repairability, Struct. Des. Tall Spec. Build. 25 (2016) 93–111. https://doi.org/10.1002/tal.1230.

[5] J.F. Hajjar, A.H. Sesen, E. Jampole, A. Wetherbee, A synopsis of sustainable structural systems with Rocking,Self-Centering,and Articulated Energy-Dissipating Fuses, J. Earthq. Eng. 10 (2013) 45–66.

[6] T. Takeuchi, X. Chen, R. Matsui, Seismic performance of controlled spine frames with energy-dissipating members, J. Constr. Steel Res. 114 (2015) 51–65. https://doi.org/10.1016/j.jcsr.2015.07.002.

[7] A. Abdolahi Rad, Seismic ratcheting of steel low-damage buildings, University of Canterbury, 2017. https://doi.org/10.26021/1702.

[8] M. Grigorian, Resiliency and post-earthquake realignment, Struct. Des. Tall Spec. Build. 30 (2021) e1836. https://doi.org/10.1002/tal.1836.

[9] M. Grigorian, A.S. Moghadam, H. Mohammadi, M. Kamizi, Methodology for developing earthquake-resilient structures, Struct. Des. Tall Spec. Build. 28 (2018) e1571. https://doi.org/10.1002/tal.1571.

[10] G.W. Housner, The behavior of inverted pendulum structures during earthquakes, Bull. Seismol. Soc. Am. 53 (1963) 403–417. https://doi.org/10.1017/CBO9781107415324.004.

[11] R.W. Clough, A.A. Huckelbridge, Preliminary experimental study of seismic uplift of a steel frame, Earthq. Eng. Res. Cent. (1977) Report No. UCB/EERC-77/22.

[12] J.I. Restrepo, J. Mander, T.J. Holden, New Generation of Structural Systems for Earthquake Resistance, in: New Zeal. Soc. Earthq. Eng. 2001 Conf., 2001: pp. 1–9.

[13] X. Lu, X. Dang, J. Qian, Y. Zhou, H. Jiang, Experimental Study of Self-Centering Shear Walls with Horizontal Bottom Slits, J. Struct. Eng. 143 (2017) 04016183. https://doi.org/10.1061/(asce)st.1943-541x.0001673.

[14] M.H. Mohammadi, A. Massumi, A. Meshkat-Dini, Performance of RC moment frames with fixed and hinged supports under near-fault ground motions, Earthq. Struct. 13 (2017) 89–101. https://doi.org/10.12989/eas.2017.13.1.089.

[15] M. Grigorian, A.S. Moghadam, H. Mohammadi, Advances in rocking core-moment frame analysis, Bull. Earthq. Eng. 15 (2017) 5551–5577. https://doi.org/10.1007/s10518-017-0177-8.

[16] A. Massumi, N. Karimi, M. Ahmadi, Effects of openings geometry and relative area on seismic performance of steel shear walls, Steel Compos. Struct. 28 (2018) 617–628. https://doi.org/10.12989/scs.2018.28.5.617.

[17] F.C. Blebo, D.A. Roke, Seismic-resistant self-centering rocking core system with buckling restrained columns, Eng. Struct. 173 (2018) 372–382. https://doi.org/10.1016/j.engstruct.2018.06.117.

[18] X. Hu, Q. Lu, Y. Yang, Rocking Response Analysis of Self-Centering Walls under Ground Excitations, Math. Probl. Eng. 2018 (2018) 1–12. https://doi.org/10.1155/2018/4371585.

[19] C.P. Lin, R. Wiebe, J.W. Berman, Analytical and numerical study of curved-base rocking walls, Eng. Struct. 197 (2019) 109397. https://doi.org/10.1016/j.engstruct.2019.109397.

[20] D. Wu, X. Lu, B. Zhao, Parametric study of rocking cores-moment frames with supplemental viscous damping and self-centering devices using a distributed parameter model, Soil Dyn. Earthq. Eng. 123 (2019) 304–319. https://doi.org/10.1016/j.soildyn.2019.04.034.

[21] H.-E. Blomgren, S. Pei, Z. Jin, J. Powers, J.D. Dolan, J.W. van de Lindt, A.R. Barbosa, D. Huang, Full-Scale Shake Table Testing of Cross-Laminated Timber Rocking Shear Walls with Replaceable Components, J. Struct. Eng. 145 (2019) 04019115. https://doi.org/10.1061/(asce)st.1943-541x.0002388.

[22] Q. Xie, Z. Zhou, S.P. Meng, Experimental investigation of the hysteretic performance of self-centering buckling-restrained braces with friction fuses, Eng. Struct. 203 (2020) 109865. https://doi.org/10.1016/j.engstruct.2019.109865.

[23] J. Li, W. Wang, B. Qu, Seismic design of low-rise steel building frames with self-centering panels and steel strip braces, Eng. Struct. 216 (2020) 110730. https://doi.org/10.1016/j.engstruct.2020.110730.

[24] Z. Li, F. Chen, M. He, R. Zhou, Y. Cui, Y. Sun, G. He, Lateral Performance of Self-Centering Steel–Timber Hybrid Shear Walls with Slip-Friction Dampers: Experimental Investigation and Numerical Simulation, J. Struct. Eng. 147 (2021) 04020291. https://doi.org/10.1061/(asce)st.1943-541x.0002850.

[25] S. Hu, W. Wang, M.S. Alam, B. Qu, Performance-based design of self-centering energy-absorbing dual rocking core system, J. Constr. Steel Res. 181 (2021) 106630. https://doi.org/10.1016/j.jcsr.2021.106630.

[26] E. Elettore, F. Freddi, M. Latour, G. Rizzano, Design and analysis of a seismic resilient steel moment resisting frame equipped with damage-free self-centering column bases, J. Constr. Steel Res. 179 (2021) 106543. https://doi.org/10.1016/j.jcsr.2021.106543.

[27] S. Mazzoni, F. McKenna, M.H. Scott, G.L. Fenves, OpenSees command language manual, Pacific Earthq. Eng. Res. Cent. 264 (2006) 451.

[28] B. Qu, J.C. Sanchez, H. Hou, M. Pollino, Improving inter-story drift distribution of steel moment resisting frames through stiff rocking cores, Int. J. Steel Struct. 16 (2016) 547–557. https://doi.org/10.1007/s13296-016-6023-z.

[29] A. Gupta, H. Krawinkler, Seismic Demands for Performance Evaluation of Steel, Stanford University, 1999.

[30] A. Committee, Specification for structural steel buildings (ANSI/AISC 360-10), Am. Inst. Steel Constr. Chicago-Illinois. (2010).

[31] Building and Housing Research Center (BHRC), Iranian Code of Practice for seismic resistant design of buildings. Standard No. 2800, 4th ed., Build. Hous. Res. Cent. (2015).

[32] A.S. of C.E. (ASCE), ASCE Standard–ASCE/SEI 7–16: Minimum Design Loads for Buildings and Other Structures, (2016).

[33] Pacific Earthquake Engineering Research Center.(PEER), PEER Ground Motion Database, Shallow Crustal Earthquakes Act. Tecton. Regimes, NGA-West2. (2013). http://ngawest2.berkeley.edu/.

[34] U.B. Code, Structural engineering design provisions, in: Int. Conf. Build. Off., 1997.

[35] R. Pekelnicky, C. Poland, ASCE 41-13: Seismic Evaluation and Retrofit Rehabilitation of Existing Buildings, SEAOC 2012 Conv. Proc. (2012).

[36] T. Paulay, M.J.N. Priestley, Seismic design of reinforced concrete and masonry buildings, (1992).

[37] D. Vamvatsikos, C.A. Cornell, Incremental dynamic analysis, Earthq. Eng. Struct. Dyn. 31 (2002) 491–514.

[38] D. Vamvatsikos, C.A. Cornell, Applied incremental dynamic analysis, Earthq. Spectra. 20 (2004) 523–553. https://doi.org/10.1193/1.1737737.